Journal of Medical Microbiology and Infectious Diseases

JoMMID
ISSN: 2345-5349
eISSN: 2345-5330

Bioactive Potential and HR-LC-MS Analysis of *Malbranchea cinnamomea* Extract

Madhuri Peethala[1], Shanthipriya Ajmera[1*], Divya Ajmeera[2], Sandeepta Burgula[3]

[1]Department of Microbiology, Palamuru University, Mahabubnagar 509001, Telangana, India; [2]Department of Cell Biology, ICMR-National Institute of Nutrition, Hyderabad 500007, Telangana, India; [3]Department of Microbiology, Osmania University, Hyderabad 500007, Telangana, India

ARTICLE INFO

Original Article

Keywords: Antimicrobial resistance, Bioactive metabolites, Drug discovery, HR-LC-MS, *Malbranchea cinnamomea*, Thermophilic fungi

Received: 02 Sep. 2025
Received in revised form: 24 May. 2026
Accepted: 03 Aug. 2026
DOI: 10.61882/JoMMID.14.2.87

***Correspondence**
Email:
drspajmera@palamuruuniversity.ac.in

© The Author(s)

ABSTRACT

Introduction: Thermophilic coprophilous fungi inhabiting nutrient-rich environments with intense microbial competition, such as *Malbranchea cinnamomea*, remain underexplored as sources of bioactive secondary metabolites. Therefore, this study aimed to evaluate the bioactive potential of *M. cinnamomea* ethyl acetate crude extract. **Methods:** *M. cinnamomea* was isolated from herbivore dung (goat, cattle, and sheep) and cultivated via submerged fermentation. The ethyl acetate crude extract was assessed for antibacterial activity against *Staphylococcus aureus* MTCC 96 via the agar well diffusion assay, cytotoxicity in RAW 264.7 murine macrophage cells using the MTT assay, and hemolytic potential through an erythrocyte lysis assay. Additional screening evaluated activity against *Mycobacterium tuberculosis*, *Plasmodium falciparum*, and dengue virus serotype 2 (DENV-2), along with cytotoxicity testing in Vero cells. Preliminary chemical characterization was performed using thin-layer chromatography (TLC), Fourier-transform infrared (FTIR) spectroscopy, and high-resolution liquid chromatography-mass spectrometry (HR-LC-MS). **Results:** The extract exhibited concentration-dependent cytotoxicity against RAW 264.7 cells (IC_{50} = 14.9 ± 0.1 µg/mL) and antibacterial activity against *S. aureus*, with inhibition zones of 37.7 ± 1.1 mm at 90 µg/mL. Hemolysis remained below 20% across tested concentrations, indicating low hemolytic potential. Screening showed negligible activity against *M. tuberculosis*, *P. falciparum*, and DENV-2, and no cytotoxicity was observed in Vero cells (CC_{50} > 1000 µg/mL). TLC revealed multiple components, FTIR revealed diverse functional groups, and HR-LC-MS detected six putative fungal metabolites including lipid derivatives, peptides, and phenolic compounds. **Conclusion:** *M. cinnamomea* produces chemically diverse secondary metabolites exhibiting antibacterial activity, concentration-dependent cytotoxicity against RAW 264.7 macrophages, and low hemolytic potential. These findings support further bioassay-guided fractionation and chemical characterization to identify novel bioactive compounds.

INTRODUCTION

Antimicrobial resistance (AMR) and cancer represent major global health challenges, underscoring the urgent need for novel antimicrobial and anticancer agents with improved efficacy, specificity, and safety profiles [1–3]. In this context, natural products remain a cornerstone of drug discovery due to their structural diversity and evolutionary optimization, often conferring superior biological selectivity and target compatibility relative to purely synthetic compounds [4, 5].

Among natural sources, thermophilic coprophilous fungi inhabiting nutrient-rich ecological niches such as herbivore dung, characterized by intense microbial competition, are increasingly recognized as underexplored producers of chemically diverse secondary metabolites [6, 7]. Their thermophilic adaptation is particularly relevant to drug discovery, as organisms thriving at elevated temperatures often produce metabolites with enhanced structural stability and resistance to degradation, properties that are highly advantageous for pharmacological development [8]. Coupled with intense ecological competition, these conditions promote the evolution of bioactive compounds exhibiting antimicrobial and cytotoxic activities.

Malbranchea cinnamomea is a thermophilic ascomycete reported to produce malbranchein, a quinone-derived

[Downloaded from jommid.pasteur.ac.ir on 2026-11-25]

[DOI: 10.61882/JoMMID.14.2.87]

antibiotic with antimicrobial and cytotoxic activity against selected bacterial strains and cancer cell lines [6]. However, beyond malbranchein, the chemical diversity and pharmacological potential of *M. cinnamomea* remain poorly characterized [8]. In particular, limited information exists regarding the antibacterial activity of its ethyl acetate crude extract, cytotoxic effects in mammalian cell models, hemocompatibility, and overall safety profile.

To address these knowledge gaps, the present study systematically evaluated the pharmacological potential of *M. cinnamomea* ethyl acetate crude extract through antibacterial, cytotoxic, and hemolytic assays, complemented by screening against selected pathogens (*Mycobacterium tuberculosis*, *Plasmodium falciparum* and dengue virus serotype 2 (DENV-2)), and mammalian cell models (Vero cells). Preliminary chemical characterization was conducted using thin-layer chromatography (TLC), Fourier-transform infrared (FTIR) spectroscopy, and high-resolution liquid chromatography-mass spectrometry (HR-LC-MS) to gain insight into the chemical constituents contributing to the observed bioactivity. This integrated approach aimed to assess *M. cinnamomea* as a thermophilic fungal source of pharmacologically relevant secondary metabolites for future drug discovery efforts targeting AMR and broader therapeutic applications.

MATERIAL AND METHODS

Chemicals and reagents. Culture media components (yeast extract and sucrose) and commercially prepared, ready-to-use media, including Sabouraud dextrose agar (SDA) and Mueller–Hinton agar (MHA), were obtained from HiMedia Laboratories (Mumbai, India). Organic solvents such as ethyl acetate, methanol, chloroform, hexane, and glacial acetic acid were of analytical grade. Reagents including sodium dodecyl sulfate (SDS), dimethyl sulfoxide (DMSO), streptomycin discs (10 µg), and rifampicin were also procured from HiMedia Laboratories. The reagents 3-(4,5-dimethylthiazol-2-yl)-2,5-diphenyltetrazolium bromide (MTT), paclitaxel, chloroquine, ribavirin, doxorubicin, resazurin sodium salt, and SYBR Green I were purchased from Sigma-Aldrich (St. Louis, MO, USA). Potassium bromide (KBr) used for FTIR spectroscopy was obtained from Merck (Darmstadt, Germany). All solvents used for chromatographic and HR-LC-MS analyses were of HPLC grade. Ultrapure water (Milli-Q water system, Merck Millipore, 18.2 MΩ·cm) was used throughout the experiments.

Microbial strains and fungal isolate. The thermophilic fungal isolate used in this study was identified as *M. cinnamomea* through morphological and molecular characterization. The partial internal transcribed spacer (ITS) sequence of the isolate was deposited in GenBank under accession number PX944829 (submission ID SUB15980959; strain code MC6; Supplementary Material 1). *Staphylococcus aureus* MTCC 96 was obtained from the Microbial Type Culture Collection (MTCC, Chandigarh, India) and maintained on MHA slants at 4°C with periodic subculturing. *M. tuberculosis* H37Ra (ATCC 25177) was obtained from a certified national reference laboratory in India and cultured in Middlebrook 7H9 broth supplemented with oleic acid-albumin-dextrose-catalase (OADC) enrichment under biosafety level 2 (BSL-2) conditions. The identities of the bacterial strains were confirmed using standard biochemical tests prior to experimentation.

Parasitic and viral models. *Plasmodium falciparum* strain 3D7 was maintained in human O-positive erythrocytes using RPMI-1640 medium supplemented with heat-inactivated (56°C for 30 min) pooled human serum under standard *in vitro* culture conditions within a BSL-2 laboratory. Dengue virus serotype 2 (DENV-2, New Guinea C strain) was propagated in Vero cells cultured in Dulbecco's Modified Eagle Medium (DMEM) supplemented with 2% fetal bovine serum (FBS) and maintained at 37°C in a humidified 5% CO_2 atmosphere under BSL-2 containment.

Cell lines and culture conditions. RAW 264.7 murine macrophages and Vero (African green monkey kidney epithelial) cells were obtained from the National Centre for Cell Science (NCCS, Pune, India). The cells were cultured in DMEM supplemented with 10% FBS and penicillin–streptomycin (100 U/mL and 100 µg/mL, respectively) at 37°C in a humidified incubator with 5% CO_2. They were subcultured upon reaching 70–80% confluence and maintained below passage 20 to ensure phenotypic stability.

Blood samples for the hemolytic assay. Fresh rabbit blood samples were collected into ethylenediaminetetraacetic acid (EDTA)-coated vacuum tubes via standard venipuncture techniques without anesthesia. Samples were processed within 2 h of collection to maintain sample integrity.

Ethical approval. All experimental procedures involving animal-derived materials were reviewed and approved by the Institutional Animal Ethics Committee (IAEC; approval number 31/IAEC-II/SLSPL/2024) and conducted in compliance with the Committee for the Purpose of Control and Supervision of Experiments on Animals (CPCSEA) guidelines and institutional protocols.

Instrumentation. Laboratory instruments used included a laminar airflow cabinet, a CO_2 incubator, a rotary evaporator, a UV–visible spectrophotometer, an FTIR spectrometer, and a microplate reader. HR-LC-MS analysis was performed using an Agilent 6545 Q-TOF LC-MS system equipped with an Agilent ZORBAX Eclipse Plus C18 column (2.1 mm × 100 mm, 1.7 µm). TLC was conducted using silica gel 60 F_{254} plates (20 × 20 cm, a thickness of 0.25 mm; Merck, Darmstadt, Germany).

Software and databases. HR-LC-MS data acquisition and processing were performed using Agilent MassHunter software for 6200 Series TOF/6500 Series Q-TOF systems (version B.05.01, build B5125.3, Agilent Technologies, Santa Clara, CA, USA). Compound annotation was conducted using the METLIN database and the Global Natural Products Social Molecular Networking (GNPS) platform.

[Downloaded from jommid.pasteur.ac.ir on 2026-11-25]

[DOI: 10.61882/JoMMID.14.2.87]

Fungal isolation and identification. Fresh dung samples (n = 15) were aseptically collected from goats, cattle, and sheep in Telangana, India, during the summer of 2022. Samples were collected in sterile plastic bags, transported to the laboratory at ambient temperature, and processed within 24 h of collection. The collected samples were serially diluted (10^{-1} to 10^{-4}) and plated onto yeast extract-sucrose (YES) agar and incubated at 45°C for 5 days under aerobic conditions to selectively isolate thermophilic fungi [9]. A total of 11 thermophilic fungal isolates were obtained, subcultured, and preserved on SDA slants at 4°C with periodic subculturing every 4 weeks to maintain viability until further use [10]. Of these, *M. cinnamomea* exhibited relatively robust growth and culture stability under laboratory incubation conditions and was therefore selected for further investigations.

Molecular identification and phylogenetic analysis. Genomic DNA was extracted from fungal mycelium using the cetyltrimethylammonium bromide (CTAB) method described by Doyle and Doyle [11]. The ITS region of ribosomal DNA was amplified using universal primers ITS1 (5′-TCCGTAGGTGAACCTGCGG-3′) and ITS4 (5′-TCCTCCGCTTATTGATATGC-3′) [12]. Polymerase chain reaction (PCR) was performed in a final reaction volume of 25 µL containing 1× PCR buffer, 1.5 mM $MgCl_2$, 0.2 mM of each deoxynucleotide triphosphate (dNTP), 0.5 µM of each primer, 1 U of Taq DNA polymerase, and approximately 50 ng of template DNA. PCR amplification was carried out using a thermal cycler (Bio-Rad, Hercules, CA, USA). Thermal cycling conditions consisted of an initial denaturation at 95°C for 5 min, followed by 35 cycles of denaturation at 95°C for 30 s, annealing at 55°C for 30 s, and extension at 72°C for 1 min, with a final extension at 72°C for 7 min.

PCR products were purified and sequenced using the Sanger dideoxy sequencing method on a 3500 Genetic Analyzer (Applied Biosystems, Foster City, CA, USA) [13]. Raw chromatograms (.ab1 files) were manually inspected; low-quality ends were trimmed, and forward and reverse sequences were assembled into consensus sequences using MEGA software (version 11). The consensus ITS sequence was subjected to nucleotide Basic Local Alignment Search Tool (BLASTn) analysis against the National Center for Biotechnology Information (NCBI) GenBank database for taxonomic identification.

For phylogenetic analysis, ITS sequences of closely related taxa retrieved from GenBank were aligned using the MUSCLE algorithm implemented in MEGA software. A neighbor-joining (NJ) phylogenetic tree was constructed using the Tamura–Nei substitution model with 1,000 bootstrap replicates to assess branch support. Sequences of *Gymnoascus* spp. were used as the outgroup to root the tree due to their phylogenetic proximity to *Malbranchea* within the family Onygenaceae. Bootstrap values ≥ 50% were considered significant and were shown at the nodes. The isolate, designated MC6, clustered with reference *M. cinnamomea* strains, confirming species-level identity.

Submerged fermentation and extraction. *M. cinnamomea* was cultured in 500 mL Erlenmeyer flasks containing 250 mL of YES broth (yeast extract 20 g/L, sucrose 150 g/L, pH adjusted to 7.0; autoclaved at 121°C for 15 min). Fermentation was initiated by inoculating each flask with three agar plugs (6-mm diameter) excised from actively growing 5-day-old SDA cultures. The cultures were incubated at 50°C under static conditions for 15 days to promote secondary metabolite production. Three biological replicates were processed independently to ensure reproducibility, and an uninoculated YES broth control was processed in parallel under identical conditions.

Following incubation, the cultures were filtered through Whatman No. 1 filter paper under vacuum to separate mycelial biomass. The filtrate was extracted three times with equal volumes of ethyl acetate, and the combined organic layers were dried over anhydrous sodium sulfate, filtered, and concentrated under reduced pressure using a rotary evaporator at 40°C to obtain the crude extract [14–17]. The extraction yield was determined gravimetrically and expressed as mg/100 mL of culture filtrate.

Cytotoxicity assay. The cytotoxic effect of the *M. cinnamomea* crude extract was evaluated using the MTT assay on RAW 264.7 murine macrophage cells [18]. Cells were seeded in 96-well plates at a density of 1×10^4 cells/well in complete DMEM and incubated for 18–24 h at 37°C in a humidified 5% CO_2 atmosphere to allow attachment. Cells were then treated with the extract at final concentrations of 2.5, 5, 10, 25, 50, and 100 µg/mL for 24 h. MTT (0.5 mg/mL final concentration) was added and incubated for 4 h. Formazan crystals were dissolved in DMSO, and absorbance was measured at 570 nm (reference 630 nm). The vehicle control contained ≤ 0.5% (*v/v*) DMSO. Cell viability was calculated relative to untreated controls, and IC_{50} values were determined using nonlinear regression analysis (GraphPad Prism). Data are expressed as mean ± SD from three independent experiments, each performed in triplicate. Paclitaxel (0.01–10 µg/mL) served as the positive control.

Antibacterial activity (agar well diffusion assay). The antibacterial activity of *M. cinnamomea* crude extract was evaluated against *S. aureus* MTCC 96 using the agar well diffusion method following Clinical and Laboratory Standards Institute (CLSI) guidelines [19]. MHA plates were inoculated with a 0.5 McFarland standardized bacterial suspension (≈1.5×10^8 colony-forming units (CFU)/mL). Wells (7 mm diameter) were prepared and filled with extract solutions adjusted to yield final concentrations of 25, 50, and 90 µg/mL. Streptomycin (10 µg/ disc) served as the positive control, while DMSO was used as the negative control. Plates were incubated at 37°C for 24 h, and inhibition zones were measured in millimeters (including well diameter). All experiments were performed in triplicate.

Hemolytic activity. The hemolytic potential of the crude extract was evaluated using an erythrocyte lysis assay as previously described with minor modifications [20, 21]. Fresh blood samples were collected from healthy rabbits.

[Downloaded from jommid.pasteur.ac.ir on 2026-11-25]

[DOI: 10.61882/JoMMID.14.2.87]

Erythrocytes were separated by centrifugation at 1000 × g for 5 min, washed twice with phosphate-buffered saline (PBS) (pH 7.4), and resuspended in PBS to obtain a 1% (*v/v*) erythrocyte suspension. The crude extract, dissolved in DMSO and diluted in PBS, was tested at concentrations of 2.5, 5, 10, 25, 50, and 100 µg/mL, with final DMSO concentrations not exceeding 0.5% (*v/v*). Equal volumes of erythrocyte suspension (100 µL) and extract solution (100 µL) were mixed and incubated at 37°C for 24 h under static conditions. After incubation, samples were centrifuged at 1000 × g for 5 min, and the absorbance of the supernatant was measured at 540 nm to quantify hemoglobin release.

PBS-suspended erythrocytes served as the negative control, while erythrocytes treated with 1% (*w/v*) SDS served as the positive control. Percentage hemolysis was calculated using Equation in below:

$$\text{Hemolysis (\%)} = \frac{A_{\text{sample}} - A_{\text{negative control}}}{A_{\text{positive control}} - A_{\text{negative control}}} \times 100$$

All assays were performed in triplicate across three independent experiments, and results are expressed as mean ± SD. Hemolysis below 10% was considered negligible, while values below 20% were considered indicative of low hemolytic potential [20, 21].

TLC analysis. Preliminary screening of the crude extract was performed using TLC on silica gel 60 F_{254} plates following the method of Wagner and Bladt [22]. The crude extract (10 mg/mL in methanol) was applied to the plates as 5 µL spots using a capillary tube approximately 1 cm from the bottom edge. Two solvent systems were used: chloroform: methanol (9:1, *v/v*) and ethyl acetate: hexane: glacial acetic acid (4:2:1, *v/v/v*). Plates were developed in a presaturated glass chamber (15 min saturation) to a distance of approximately 8 cm and air-dried before visualization. Developed plates were first visualized under short-wave (254 nm) and long-wave (366 nm) ultraviolet (UV) illumination, and then subjected to derivatization with anisaldehyde–sulfuric acid reagent prepared as described by Wagner and Bladt [22], followed by heating at 105°C for 5–10 min to enhance spot detection. Spots appeared as distinct colored bands depending on the compound classes. Rf values of each spot were calculated using the standard formula and recorded for both solvent systems as following.

$$\text{Rf} = \frac{\text{Distance traveled by spot}}{\text{Distance travelled by solvent front}}$$

FTIR spectroscopy. Functional groups in the crude extract were identified using an FTIR spectrometer (Shimadzu IR Affinity-1, Kyoto, Japan). Samples were prepared using the KBr pellet method by mixing approximately 1–2 mg of crude extract with 100 mg of anhydrous KBr, grinding thoroughly, and compressing into a transparent pellet. A background spectrum was recorded using a pure KBr pellet, and sample spectra were recorded over the range 4000–400 cm^{-1} at a resolution of 4 cm^{-1} with 32 scans per sample to enhance the signal-to-noise ratio. Functional groups were assigned according to standard FTIR spectral correlation references [23, 24].

HR-LC-MS analysis. The crude extract (1 mg/mL in methanol, filtered through a 0.22 µm polytetrafluoroethylene (PTFE) membrane filter) was analyzed using an Agilent 6545 Q-TOF LC-MS system (Agilent Technologies, Santa Clara, CA, USA) equipped with an Agilent ZORBAX Eclipse Plus C18 column (2.1 mm × 100 mm, 1.7 µm). The mobile phase consisted of solvent A (0.1% formic acid in water) and solvent B (acetonitrile). The gradient program was as follows: initial hold at 5% B for 2 min, linear increase from 5% to 95% B over 20 min, hold at 95% B for 3 min, followed by equilibration at 5% B for 5 min. Analyses were performed at a flow rate of 0.3 mL/min, column temperature of 35°C, and injection volume of 10 µL.

Mass spectra were acquired in positive electrospray ionization (ESI^+) mode over an m/z range of 100–1200, with a capillary voltage of 3500 V, a fragmentor voltage of 175 V, a drying gas flow of 10 L/min, and a drying gas temperature of 300°C. Data were processed using Agilent MassHunter software (version B.05.01), and metabolites were putatively annotated through comparison with the METLIN database [25] and the GNPS platform [26]. Only positive ion mode was used; potential underrepresentation of acidic metabolites is explained in the Discussion section.

Supplementary bioactivity evaluation. The *M. cinnamomea* crude extract was evaluated for antimycobacterial activity against *M. tuberculosis* H37Ra, antimalarial activity against *P. falciparum* 3D7, antiviral activity against DENV-2 in Vero cells, and cytotoxicity in Vero cells using standard *in vitro* assay protocols described in the subsequent sections. Positive controls were included at defined concentrations: rifampicin (2 µg/mL) for antimycobacterial assays, chloroquine (1 µM) for antimalarial assays, ribavirin (10 µg/mL) for antiviral assays, and doxorubicin (1 µM) for cytotoxicity assays. All experiments were performed in triplicate, and data are expressed as mean ± SD.

Antimalarial activity. The assay was conducted against *P. falciparum* strain 3D7 using a SYBR Green I fluorescence-based method [27]. Parasite cultures (1% parasitemia, 2% hematocrit) containing synchronized ring-stage parasites obtained by 5% sorbitol treatment for 5 h were incubated with serial dilutions of the extract (5, 10, 25, 50, 100, 250, and 500 µg/mL) for 48–72 h at 37°C under microaerophilic conditions (5% CO_2, 5% O_2, 90% N_2). Parasite growth inhibition was quantified by measuring fluorescence intensity following SYBR Green I staining, and IC_{50} values were calculated using GraphPad Prism software. Data are expressed as the mean ± SD from three independent experiments, each performed in triplicate. Chloroquine (1 µM) served as the positive control and exhibited expected concentration-dependent inhibition.

Antiviral activity. The activity of the extract against DENV-2 was evaluated using a flow cytometry-based virus reduction assay [28]. Vero cells infected with DENV-2 at a multiplicity of infection (MOI) of 0.1 were treated with extract concentrations of 10–500 µg/mL following a 2h viral adsorption period.

[Downloaded from jommid.pasteur.ac.ir on 2026-11-25]

[DOI: 10.61882/JoMMID.14.2.87]

After 48–72 h of incubation, viral replication was quantified by measuring dengue virus envelope antigen expression using an anti-dengue virus envelope protein monoclonal antibody (clone 4G2, Merck Millipore) followed by flow cytometric analysis. Data are expressed as the mean ± SD from three independent experiments, each performed in triplicate. Ribavirin (10 µg/mL) served as the positive control and exhibited expected inhibition of viral replication.

Cytotoxicity in Vero cells. Vero cells were seeded at a density of 1 × 10^4 cells per well in 96-well plates and allowed to attach for 18–24 h at 37°C in a humidified 5% CO_2 atmosphere. Cells were treated with the extract at concentrations ranging from 10 to 1000 µg/mL for 24 h. Cell viability was determined using the MTT assay as described for RAW 264.7 cells, and half-maximal cytotoxic concentration (CC_{50}) values were calculated using concentration-response analysis. Data are expressed as the mean ± SD from three independent experiments, each performed in triplicate. Doxorubicin (0.1–5 µg/mL) served as the positive control and exhibited expected concentration-dependent cytotoxicity.

Statistical analysis. Statistical analyses were performed using GraphPad Prism software (version 9.5; GraphPad Software, San Diego, CA, USA). Data were analyzed using one-way analysis of variance (ANOVA) followed by Tukey's post hoc test. Results were expressed as the mean ± standard deviation (SD), and differences were considered statistically significant at $P < 0.05$.

RESULTS

Fungal identification and phylogeny. The thermophilic fungal isolate (MC6) exhibited rapid growth at 45–50°C, forming white, cottony colonies with well-defined entire margins that turned yellow upon maturation. Microscopic examination (lactophenol cotton blue staining, light microscopy at 400× magnification) revealed septate hyphae and cylindrical arthroconidia (approximately 5–8 × 3–4 µm) arising from hyphal fragmentation, consistent with the morphological features of the genus *Malbranchea*.

Molecular identification based on ITS region sequencing confirmed the isolate as *M. cinnamomea*, showing 99% sequence identity (query coverage: 100%, *E*-value: 0.0) to reference sequences (GenBank accession numbers PP951851.1, GU733363.1, and JQ305098.1). The ITS sequence of isolate MC6 was deposited in GenBank under accession number PX944829. Phylogenetic analysis placed MC6 in a strongly supported clade (bootstrap support >95%) with other *M. cinnamomea* strains, supporting species-level identification. *Gymnoascus* sp. sequences (GenBank accession numbers NG_062769.1, EU710841.1, AB015774.1, and MN995517.1) were used as the outgroup to root the tree (Figure 1).

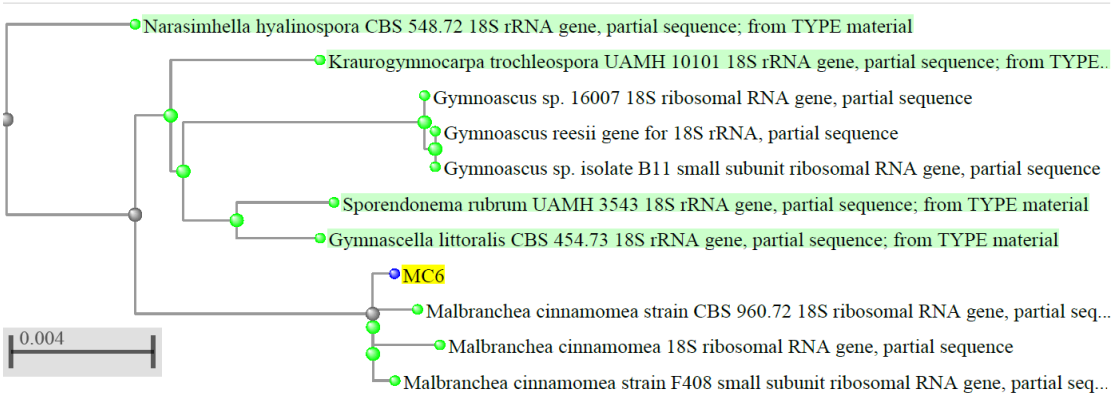


Fig. 1. Phylogenetic tree of the thermophilic fungal isolate MC6 based on ITS sequences constructed using the neighbor-joining method. Isolate MC6 clusters with *M. cinnamomea* reference sequences, confirming species-level identification. Bootstrap support values from 1,000 replicates are shown at major branch points.

Crude extract yield. Submerged fermentation of *M. cinnamomea* yielded a crude extract of 45 ± 3 mg/100 mL of culture filtrate (n = 3), confirming reproducibility across independent flasks.

Cytotoxicity assay. The *M. cinnamomea* crude extract produced a concentration-dependent reduction in RAW 264.7 murine macrophage cell viability. The IC_{50} value was 14.9 ± 0.1 µg/mL. The positive control, paclitaxel, exhibited an IC_{50} of 1.4 ± 0.2 µg/mL under identical conditions. Data are expressed as the mean ± SD from three independent experiments.

Antibacterial activity. The crude extract exhibited concentration-dependent antibacterial activity against *S. aureus* MTCC 96. At final assay concentrations of 25, 50, and 90 µg/mL, the extract produced inhibition zones of 25.1 ± 0.3 mm, 31.8 ± 1.4 mm, and 37.7 ± 1.1 mm, respectively (Figure 2). Streptomycin (10 µg/disc), used as the positive control, produced an inhibition zone of 19.2 ± 0.3 mm, while the solvent control showed no detectable activity. All tested concentrations demonstrated statistically significant antibacterial activity compared with the negative control ($P < 0.05$). The results indicated a clear concentration-dependent increase in antibacterial efficacy.

[Downloaded from jommid.pasteur.ac.ir on 2026-11-25]

[DOI: 10.61882/JoMMID.14.2.87]

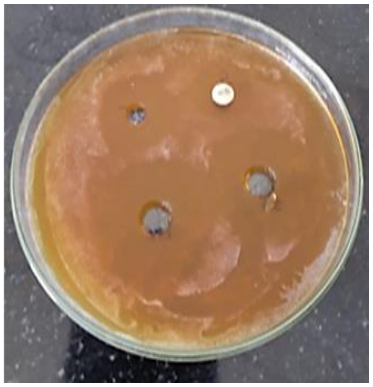


Fig. 2. Antibacterial activity of the *M. cinnamomea* crude extract against *S. aureus* MTCC 96 using the agar well diffusion assay.

The extract was tested at final concentrations of 25, 50, and 90 µg/mL. Streptomycin (10 µg/disc) served as the positive control, and DMSO served as the negative control. Plates were incubated at 37°C for 24 h. Values are expressed as the mean ± SD (n = 3). Differences were statistically significant at $P < 0.05$ compared to the negative control.

Hemolytic activity. The hemolytic potential of the crude extract was evaluated using rabbit erythrocytes at final concentrations ranging from 2.5 to 100 µg/mL. The extract exhibited low hemolytic activity across all tested concentrations, with hemolysis remaining below 20% at the highest concentration (100 µg/mL). No significant hemolysis was observed at lower concentrations (≤ 25 µg/mL), where values remained below 10%, indicating negligible membrane disruption.

PBS-treated erythrocytes served as the negative control, while erythrocytes treated with 1% SDS served as the positive control, inducing complete hemolysis.

These findings indicate a favorable preliminary hemocompatibility profile for the extract.

TLC analysis. The crude extract revealed six distinct bands with Rf values ranging from 0.38 to 0.81 (Table 1). The bands were visualized under short-wave (254 nm) and long-wave (366 nm) UV illumination and after anisaldehyde-sulfuric acid derivatization, suggesting the presence of compounds with varying polarities.

Table 1. TLC profile of *M. cinnamomea* crude extract.

Band number	Rf value	UV 254 nm	UV 366 nm	Anisaldehyde-H_2SO_4 derivatization	Possible compound class*
1	0.38	Dark quenching band	Blue fluorescence	Violet spot	Polar phenolic/amide-type compound
2	0.46	Dark band	Green fluorescence	Purple spot	Moderately polar compound
3	0.53	Faint quenching	Blue fluorescence	Light violet spot	Phenolic derivative
4	0.62	Clear dark band	Yellow fluorescence	Brownish spot	Aromatic compound
5	0.74	Moderate quenching	Blue-green fluorescence	Pink spot	Lipophilic compound
6	0.81	Faint band	Weak fluorescence	Brown spot	Non-polar/aliphatic compound

* TLC analysis was performed using silica gel 60 F_{254} plates with chloroform: methanol (9:1) and ethyl acetate:hexane: acetic acid (4:2:1). Spots were visualized under UV (254 nm and 366 nm) and after anisaldehyde-sulfuric acid derivatization. Rf values indicate the presence of compounds with varying polarity. Tentative compound class assignments are based on Rf behavior and spray reagent response; identities were not confirmed by reference standards or MS/MS analysis.

FTIR analysis. The FTIR spectrum of the crude extract (Figure 3) showed characteristic absorption bands at 3332, 2102, 1638, 1410, 1111, 1016, 648, and 522 cm^{-1}.

A broad band at 3332 cm^{-1} corresponds to O-H and/or N-H stretching vibrations, indicating the possible presence of hydroxyl or amine groups. The peak at 2102 cm^{-1} may be associated with C≡C or other unsaturated functional groups. The band at 1638 cm^{-1} is attributable to C=O (amide I) and/or aromatic C=C stretching vibrations. Peaks at 1410 and 1111 cm^{-1} may correspond to O-H bending and C-O-C stretching vibrations, respectively. The peak at 1016 cm^{-1} corresponds to C-O stretching vibrations, suggesting the presence of alcohols or ethers. The bands observed at 648 and 522 cm^{-1} represent vibrations in the fingerprint region. The FTIR spectrum suggests the presence of multiple functional groups consistent with a chemically diverse mixture. Detailed peak assignments are provided in Table 2.

[Downloaded from jommid.pasteur.ac.ir on 2026-11-25]

[DOI: 10.61882/JoMMID.14.2.87]

Table 2. FTIR spectral peak assignments of *M. cinnamomea* crude extract.

Wave number (cm^{-1})*	Possible functional group	Tentative assignment
3332	O-H/N-H stretching	Hydroxyl or amine group
2102	C≡C stretching	Unsaturated group
1638	C=O/C=C stretching	Amide or aromatic group
1410	O-H bending	Phenolic group
1111	C-O-C stretching	Ether linkage
1016	C-O stretching	Alcohol/ether
648	Fingerprint region	Skeletal vibration
522	Fingerprint region	Skeletal vibration

* FTIR spectra were recorded over 4000–400 cm^{-1}. Peak assignments are tentative and based on comparison with standard infrared correlation charts; functional group interpretations indicate possible bond vibrations and do not confirm specific compounds. Bands in the conventional fingerprint region (1500–400 cm^{-1}) represent complex skeletal and framework vibrations characteristic of organic molecules.

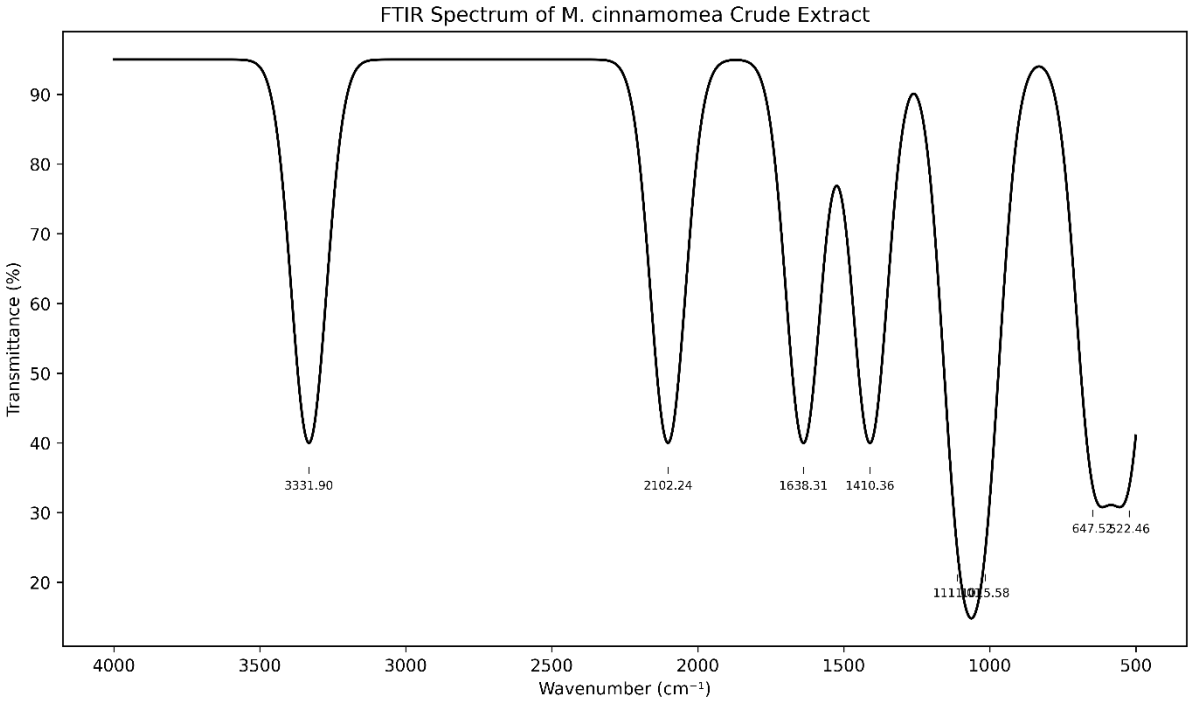


Fig. 3. FTIR spectrum of *M. cinnamomea* crude extract.

The spectrum was recorded from 4000 to 400 cm^{-1} using the KBr pellet method. Major absorption bands at 3332, 2102, 1638, 1410, 1111, 1016, 648, and 522 cm^{-1} indicate the presence of hydroxyl, amine, carbonyl, aromatic, and C-O functional groups. The assignments are based on standard infrared correlation charts.

HR-LC-MS analysis. The analysis of the crude extract was performed in ESI^+ mode. The total ion chromatogram (TIC) revealed multiple peaks corresponding to constituents present in the extract (Figure 4).

Among the detected signals, six well-resolved major peaks were selected for tentative annotation based on chromatographic separation and reproducible mass spectral signals (Table 3). The peaks were numerically labeled to correspond with the entries listed in the Table. Detailed qualitative compound reports, including MS spectra, zoomed spectra, and MS/MS peak lists for all detected compounds (Cpd 1–20), are provided in Supplementary Material 2. Tentative compound assignments were made based on accurate mass (m/z) values of protonated molecular ions $[M+H]^+$, and comparison with publicly available spectral databases, including METLIN and GNPS.

The annotated compounds included cryptophorine, cyclolaudenyl palmitate, a tripeptide (Thr-His-Trp), phenolic derivatives, and lipid-related molecules, as suggested by database matching. These identifications should be considered putative, as structural confirmation would require MS/MS fragmentation analysis, and comparison with authentic reference standards.

An additional early-eluting peak (< 1.0 min) was excluded from interpretation due to poor chromatographic resolution and irreproducible signal in ESI^+ mode. Only peaks demonstrating consistent chromatographic behavior and reliable mass spectral data were considered for annotation.

[Downloaded from jommid.pasteur.ac.ir on 2026-11-25]

[DOI: 10.61882/JoMMID.14.2.87]

Table 3. Tentatively identified metabolites from *M. cinnamomea* crude extract by HR-LC-MS (ESI^+ mode)*

Peak number	RT (min)	m/z $[M+H]^+$	Molecular formula	Tentative identification	Mass error (ppm)
1	7.70	261.21	—	Cryptophorine	<5
2	11.78	317.27	—	Lipid-related molecule	<5
3	12.17	442.19	—	Tripeptide (Thr–His–Trp)	<5
4	13.55	392.19	—	Phenolic derivative	<5
5	11.86	678.62	—	Cyclolaudenyl palmitate	<5
6	16.56	357.33	—	Lipid-related molecule	<5

* RT, retention time; m/z, mass-to-charge ratio; $[M+H]^+$, protonated molecular ion. Compound identifications are tentative and based on accurate mass comparison with spectral databases; structural confirmation using MS/MS analysis and authentic standards was not performed. One peak eluting near the void volume (<1.0 min) was excluded due to insufficient chromatographic separation.

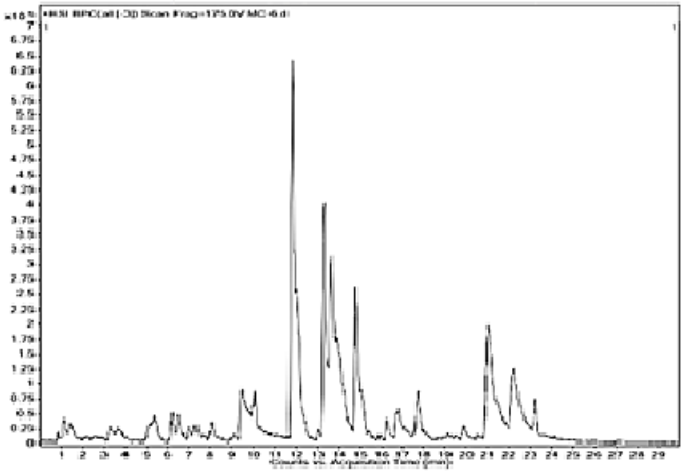


Fig. 4. HR-LC-MS total ion chromatogram (TIC) of the ethyl acetate extract of *M. cinnamomea* acquired in positive ionization mode (ESI^+).

Multiple chromatographic peaks corresponding to putative secondary metabolites were detected. Six resolved peaks were selected for tentative annotation using accurate mass (m/z) values and chromatographic retention times. Peak numbering corresponds to the compounds presented in Table 3. Peaks eluting before 1.0 min were excluded from further analysis because of insufficient chromatographic separation.

Supplementary bioactivity evaluation of MC6. The crude extract (MC6) was evaluated for antimycobacterial, antimalarial, antiviral, and cytotoxic activities to determine its preliminary biological profile. Detailed screening reports for the antimycobacterial, antimalarial, and antiviral assays, including raw fluorescence data and percentage inhibition calculations, are provided in Supplementary Material 3.

Antibacterial activity. MC6 exhibited concentration-dependent antibacterial activity against *S. aureus* MTCC 96. The inhibition zone diameters were 25.1 ± 0.3 mm, 31.8 ± 1.4 mm, and 37.7 ± 1.1 mm at 25, 50, and 90 µg/mL, respectively. Streptomycin (10 µg/disc) served as the positive control and produced an inhibition zone of 19.2 ± 0.3 mm under identical conditions.

Antimycobacterial activity. MC6 was evaluated against *M. tuberculosis* H37Ra using the resazurin microtiter assay (REMA). No inhibition of mycobacterial growth was observed at concentrations of 2.5, 5.0, and 10.0 µg/mL. Rifampicin (1 µg/mL) showed > 99% inhibition as expected. Since ≥ 90% inhibition was not achieved, MIC_{90} was determined to be >10.0 µg/mL.

Antimalarial activity. Antimalarial screening against *P. falciparum* 3D7 strain revealed < 50% inhibition at the highest concentration tested. Therefore, IC_{50} could not be determined within the tested concentration range. Chloroquine (positive control) exhibited expected inhibitory activity.

Antiviral activity and cytotoxicity. MC6 was evaluated against DENV-2 in Vero cells. The calculated parameters were IC_{50} >100 µg/mL and CC_{50} >1000 µg/mL. No measurable antiviral activity was observed, and the extract was non-cytotoxic within the tested range (Table 4).

Table 4. Summary of biological activities of *M. cinnamomea* crude extract (MC6).

Assay	Test system	Concentration range tested	Activity outcome	Key result
Antibacterial	*S. aureus* MTCC 96	25–90 µg/mL	Active (concentration-dependent)	37.7 ± 1.1 mm (90 µg/mL)
Antimycobacterial	*M. tuberculosis* H37Ra	2.5–10.0 µg/mL	Inactive	MIC_{90} >10.0 µg/mL
Antimalarial	*P. falciparum* 3D7	Up to 500 µg/mL	Inactive	<50% inhibition
Antiviral	DENV-2 (Vero cells)	Up to 100 µg/mL	Inactive	IC_{50} >100 µg/mL
Cytotoxicity	Vero cells	Up to 1000 µg/mL	Non-cytotoxic	CC_{50} >1000 µg/mL

Abbreviations: MIC_{90}: minimum inhibitory concentration required to inhibit ≥ 90% growth; IC_{50}: half-maximal inhibitory concentration; CC_{50}: half-maximal cytotoxic concentration. All values are expressed as mean ± SD. Final concentrations are reported in µg/mL. Rifampicin, chloroquine, ribavirin, and doxorubicin were used as positive controls for their respective assays.

[Downloaded from jommid.pasteur.ac.ir on 2026-11-25]

[DOI: 10.61882/JoMMID.14.2.87]

DISCUSSION

The present study investigated the chemical profile and biological activity of the crude extract from isolate *M. cinnamomea* (MC6). HR-LC-MS analysis in positive ion mode revealed six well-resolved peaks that were tentatively annotated based on accurate mass measurements and database matching. Mass errors were consistently < 5 ppm, supporting the accuracy of these provisional identifications. However, structural confirmation through MS/MS fragmentation analysis and comparison with authentic standards was not performed; therefore, compound identifications remain putative. The use of mass spectral databases for initial compound annotation is well established, although this approach carries inherent limitations when fragmentation data and reference standards are unavailable [29]. Modern metabolomics and mass spectrometry-based approaches have significantly enhanced the discovery and characterization of fungal secondary metabolites in drug research [30-32], providing a robust framework for subsequent isolation and structural elucidation of the bioactive constituents identified here.

Biological evaluation demonstrated that the MC6 extract exhibited selective antibacterial activity against *S. aureus*. The inhibition zone diameters increased in a concentration-dependent manner, indicating the presence of bioactive constituents within the crude extract. Fungal secondary metabolites are recognized as an important source of antibacterial agents, particularly against Gram-positive pathogens [33, 34]. The selective activity observed in the present study aligns with previous reports describing the susceptibility of Gram-positive bacteria to fungal-derived compounds [35]. Notably, this antibacterial activity occurred in the absence of detectable cytotoxicity in Vero cells (CC_{50} >1000 µg/mL), suggesting that the antibacterial effect is unlikely to be associated with nonspecific toxicity in this cell line. However, the extract demonstrated concentration-dependent cytotoxicity toward RAW 264.7 macrophages (IC_{50}: 14.9 ± 0.1 µg/mL), indicating cell-type-specific biological activity that warrants further investigation.

In contrast, the MC6 extract did not demonstrate detectable activity against *M. tuberculosis*, *P. falciparum*, or DENV-2 under the tested conditions. The lack of activity against these pathogens indicates selective rather than broad-spectrum antimicrobial properties. Fungal secondary metabolism is known to produce structurally diverse metabolites with specific ecological and biological functions, which may explain the observed selectivity [36-39].

This limited activity profile clarifies the pharmacological scope of the extract. Crude extracts are complex mixtures, and the concentration of active metabolites varies depending on fermentation and extraction conditions. Therefore, further investigation through bioactivity-guided fractionation and targeted screening is warranted to isolate and characterize the active constituents responsible for this activity [39].

Additionally, because HR-LC-MS analysis was conducted exclusively in ESI^+ mode, acidic and highly polar metabolites that ionize preferentially in negative ion mode may be underrepresented in the detected chemical profile. Future studies should incorporate both positive and negative ionization modes to achieve more comprehensive metabolite coverage.

A limitation of the present study is that metabolite identification was based solely on accurate mass analysis. Comprehensive structural elucidation using MS/MS fragmentation analysis, nuclear magnetic resonance (NMR) spectroscopy, and comparison with authentic standards is necessary to confirm compound identities and establish structure-activity relationships (SAR). This integrated approach is essential for advancing findings from crude extracts toward isolated lead compounds, as highlighted in contemporary natural-product drug discovery frameworks.

The *M. cinnamomea* crude extract demonstrated selective antibacterial activity against *S. aureus* while showing no detectable antimycobacterial, antimalarial, or antiviral activity under the tested conditions. The extract exhibited selective biological activity, showing concentration-dependent cytotoxicity in RAW 264.7 macrophages while remaining non-cytotoxic to Vero cells under the tested conditions.

HR-LC-MS analysis enabled tentative identification of multiple metabolites; however, further structural confirmation and bioassay-guided fractionations are required to identify the specific compounds responsible for this antibacterial activity. These findings suggest that MC6 represents a promising source of bioactive secondary metabolites and warrants further bioassay-guided fractionation, mechanistic studies, and safety evaluation.

ACKNOWLEDGEMENT

The authors thank the Council of Scientific and Industrial Research–Central Drug Research Institute (CSIR–CDRI), Lucknow, India, for facilitating supplementary biological screening assays. We also acknowledge the Sophisticated Analytical Instrument Facility/Centre for Research in Nanotechnology and Science (SAIF/CRNTS), Indian Institute of Technology Bombay, India, for providing HR-LC-MS analysis support. Palamuru University, Mahabubnagar, India, is gratefully recognized for laboratory facilities and continuous institutional support throughout the study.

CONFLICTS OF INTEREST

The authors declare that there are no conflicts of interest associated with this manuscript.

[Downloaded from jommid.pasteur.ac.ir on 2026-11-25]

[DOI: 10.61882/JoMMID.14.2.87]

FUNDING

This research received no specific grant from any funding agency in the public, commercial, or not-for-profit sectors.

DATA AVAILABILITY

All relevant data generated or analyzed during this study are included in the article and its Supplementary Information. Additional raw datasets supporting the findings of this study are available from the corresponding author upon reasonable request.

AI DISCLOSURE

The authors used large language model (LLM)-based writing assistance (ChatGPT, GPT-5 mini) to improve grammar, clarity, and language expression. All scientific content, experimental design, data analysis, interpretation, and conclusions were developed and verified by the authors.

AUTHORS' CONTRIBUTIONS

SA: Conceptualization, Supervision, Project administration. MP: Methodology, Investigation, Writing – original draft. DA: Data curation, Statistical analysis. SB: Formal analysis. All authors reviewed and approved the final manuscript.

ETHICS STATEMENT

All procedures involving rabbit whole blood were conducted in accordance with the guidelines of the CPCSEA, Government of India. The use of animal blood samples was reviewed and approved by the IAEC, Systemic Life Sciences and Research Pvt. Ltd., Hyderabad, Telangana, India, under approval number 31/IAEC-II/SLSPL/2024 (approved on 5 May 2025).

REFERENCES

1. World Health Organization. Global antimicrobial resistance and use surveillance system (GLASS) report [Internet]. Geneva: World Health Organization; 2022 [cited 2026 Jul 31]. Available from: https://www.who.int/glass

2. Murray CJL, Ikuta KS, Sharara F, Swetschinski LR, Robles Aguilar G, Lang G, et al. Global burden of bacterial antimicrobial resistance in 2019: a systematic analysis. Lancet. 2022; 399 (10325): 629–55.

3. Sung H, Ferlay J, Siegel RL, Laversanne M, Soerjomataram I, Jemal A, et al. Global cancer statistics 2020: GLOBOCAN estimates of incidence and mortality worldwide. CA Cancer J Clin. 2021; 71 (3): 209–49.

4. Newman DJ, Cragg GM. Natural products as sources of new drugs over nearly four decades from 1981 to 2019. J Nat Prod. 2020; 83 (3): 770–803.

5. Atanasov AG, Zotchev SB, Dirsch VM, Supuran CT, International Natural Product Sciences Taskforce. Natural products in drug discovery: advances and opportunities. Nat Rev Drug Discov. 2021; 20 (3): 200–16.

6. Bills GF, Gloer JB. Biologically active secondary metabolites from fungi. Nat Prod Rep. 2016; 33 (7): 790–809.

7. Wadhwa K, Kapoor N, Kaur H, Abu-Seer EA, Tariq M, Siddiqui S, et al. A comprehensive review of the diversity of fungal secondary metabolites and their emerging applications in healthcare and environment. Mycobiology. 2024; 52 (6): 335–87.

8. Turner P, Mamo G, Karlsson EN. Potential and utilization of thermophiles and thermostable enzymes in biorefining. Microb Cell Fact. 2007; 6: 9.

9. Cooney DG, Emerson R. Thermophilic fungi: an account of their biology, activities and classification. San Francisco: WH Freeman; 1964.

10. Pitt JI, Hocking AD. Fungi and food spoilage. 3rd ed. New York: Springer; 2009.

11. Doyle JJ, Doyle JL. A rapid DNA isolation procedure for small quantities of fresh leaf tissue. Phytochem Bull. 1990; 19: 11–5.

12. White TJ, Bruns T, Lee S, Taylor J. Amplification and direct sequencing of fungal ribosomal RNA genes for phylogenetics. In: Innis MA, Gelfand DH, Sninsky JJ, White TJ, editors. PCR protocols: a guide to methods and applications. San Diego: Academic Press; 1990. p. 315–22.

13. Sanger F, Nicklen S, Coulson AR. DNA sequencing with chain-terminating inhibitors. Proc Natl Acad Sci U S A. 1977; 74 (12): 5463–7.

14. Demain AL, Sanchez S. Microbial drug discovery: 80 years of progress. J Antibiot (Tokyo). 2009; 62 (1): 5–16.

15. Keller NP, Turner G, Bennett JW. Fungal secondary metabolism—from biochemistry to genomics. Nat Rev Microbiol. 2005; 3 (12): 937–47.

16. BerdY J. Bioactive microbial metabolites. J Antibiot (Tokyo). 2005; 58 (1): 1–26.

17. Nielsen JC, Nielsen J. Development of fungal cell factories for the production of secondary metabolites. Biotechnol Lett. 2017; 39 (1): 1-14.

18. Mosmann T. Rapid colorimetric assay for cellular growth and survival: application to proliferation and cytotoxicity assays. J Immunol Methods. 1983; 65 (1-2): 55–63.

19. Clinical and Laboratory Standards Institute. Performance standards for antimicrobial susceptibility testing. 33rd ed. CLSI supplement M100. Wayne, PA: CLSI; 2023.

20. Evans BC, Nelson CE, Yu SS, Beavers KR, Kim AJ, Li H, et al. *Ex vivo* red blood cell hemolysis assay for the evaluation of nanoparticle cytotoxicity. Nat Protoc. 2013; 8 (9): 1708–15.

21. Malagoli D. A full-length protocol to test hemolytic activity of compounds on human erythrocytes. MethodsX. 2016; 3: 92–7.

22. Wagner H, Bladt S. Plant drug analysis: a thin layer chromatography atlas. 2nd ed. Berlin: Springer; 1996.

23. Coates J. Interpretation of infrared spectra, a practical approach. In: Meyers RA, editor. Encyclopedia of analytical chemistry. Chichester: John Wiley & Sons; 2000. p. 10815-37.

24. Silverstein RM, Webster FX, Kiemle DJ, Bryce DL. Spectrometric identification of organic compounds. 8th ed. Hoboken: John Wiley & Sons; 2014.

[Downloaded from jommid.pasteur.ac.ir on 2026-11-25]

[DOI: 10.61882/JoMMID.14.2.87]

25. Smith CA, O'Maille G, Want EJ, Qin C, Trauger SA, Brandon TR, et al. METLIN: a metabolite mass spectral database. Ther Drug Monit. 2005; 27 (6): 747–51.

26. Wang M, Carver JJ, Phelan VV, Sanchez LM, Garg N, Peng Y, et al. Sharing and community curation of mass spectrometry data with Global Natural Products Social Molecular Networking. Nat Biotechnol. 2016; 34 (8): 828–37.

27. Smilkstein M, Sriwilaijaroen N, Kelly JX, Wilairat P, Riscoe M. Simple and inexpensive fluorescence-based technique for high-throughput antimalarial drug screening. Antimicrob Agents Chemother. 2004; 48 (5): 1803–6.

28. Diamond MS, Pierson TC. Molecular insight into dengue virus pathogenesis and its implications for disease control. Cell. 2015; 162 (3): 488–92.

29. Aron AT, Gentry EC, McPhail KL, Nothias LF, Busby B, Clark TN, et al. Reproducible molecular networking of untargeted mass spectrometry data using GNPS. Nat Protoc. 2020; 15 (4): 1954–91.

30. Wolfender JL, Marti G, Thomas A, Bertrand S. Current approaches and challenges for the metabolite profiling of complex natural extracts. J Chromatogr A. 2015; 1382: 136–64.

31. Li JW, Vederas JC. Drug discovery and natural products: end of an era or an endless frontier? Science. 2009; 325 (5937): 161–5.

32. Ayon NJ, Earp CE, Gupta R, Butun FA, Clements AE, Lee AG, et al. Bioactivity-driven fungal metabologenomics identifies antiproliferative stemphone analogs and their biosynthetic gene cluster. Metabolomics. 2024; 20(5):90

33. Demain AL. Importance of microbial natural products and the need to revitalize their discovery. J Ind Microbiol Biotechnol. 2014; 41 (2): 185–201.

34. Deshmukh SK, Prakash V, Ranjan A. Marine fungi: a source of potential antibacterial compounds. Front Microbiol. 2018; 9: 170.

35. Hyde KD, Xu J, Rapior S, Jeewon R, Lumyong S, Ngee-Ahing T, et al. The amazing potential of fungi: 50 ways we can exploit fungi industrially. Fungal Divers. 2019; 97 (1): 1-136.

36. Keller NP. Fungal secondary metabolism: regulation, function and drug discovery. Nat Rev Microbiol. 2019; 17 (3): 167–80.

37. Gonçalves MF, Esteves AC, Alves A. Fungal secondary metabolites: ecological functions and applications. Appl Microbiol Biotechnol. 2023; 107 (2-3): 995–1012.

38. Prakash S, Kumari H, Sinha M, Kumar A. Regulation and induction of fungal secondary metabolites: a comprehensive review. Arch Microbiol. 2025;207(8):189

39. Harvey AL, Edrada-Ebel R, Quinn RJ. The re-emergence of natural products for drug discovery in the genomics era. Nat Rev Drug Discov. 2015; 14 (2): 111–9.

Cite this article:
Peethala M, Ajmera S, Ajmeera D, Burgula S. Bioactive potential and HR-LC-MS analysis of *Malbranchea cinnamomea* extract. J Med Microbiol Infect Dis. 2026; 14 (2): 87-97. DOI: 10.61882/JoMMID.14.2.87.

[Downloaded from jommid.pasteur.ac.ir on 2026-11-25]

[DOI: 10.61882/JoMMID.14.2.87]